The ER-localized Ca^{2+}-binding protein calreticulin couples ER stress to autophagy by associating with microtubule-associated protein 1A/1B light chain 3

Received for publication, August 2, 2018, and in revised form, November 11, 2018 Published, Papers in Press, November 14, 2018, DOI 10.1074/jbc.RA118.005166

Yunzhi Yang[1], **Fengguang Ma**[1], **Zhengshuai Liu, Qian Su, Yuxiao Liu, Zhixue Liu, and Yu Li**[2]

From CAS Key Laboratory of Nutrition, Metabolism, and Food Safety, Shanghai Institute of Nutrition and Health, Shanghai Institutes for Biological Sciences, University of the Chinese Academy of Sciences, Chinese Academy of Sciences, Shanghai 200031, China

Edited by Ursula Jakob

Autophagy is of key importance for eliminating aggregated proteins during the maintenance of cellular proteostasis in response to endoplasmic reticulum (ER) stress. However, the upstream signaling that mediates autophagy activation in response to ER stress is incompletely understood. In this study, *in vivo* and *in vitro* approaches were utilized that include gain- and loss-of-function assays and mouse livers and human cell lines with tunicamycin-induced pharmacological ER stress. We report that calreticulin, a quality control chaperone that binds to misfolded glycoproteins for refolding in the ER, is induced under ER stress. Calreticulin overexpression stimulated the formation of autophagosomes and increased autophagic flux. Interestingly, calreticulin was sufficient for attenuating ER stress in tunicamycin- or thapsigargin-treated HeLa cells, whereas lentivirus-mediated shRNA calreticulin knockdown exacerbated ER stress. Mechanistically, we noted that calreticulin induces autophagy by interacting with microtubule-associated protein 1A/1B-light chain 3 (LC3). Confocal microscopy revealed that the colocalization of calreticulin and LC3 at the autophagosome was enhanced under ER stress conditions. Importantly, a conserved LC3-interacting region was necessary for calreticulin-mediated stimulation of autophagy and for reducing ER stress. These findings indicate a calreticulin-based mechanism that couples ER stress to autophagy activation, which, in turn, attenuates cellular stress, likely by alleviating the formation of aberrantly folded proteins. Pharmacological or genetic approaches that activate calreticulin–autophagy signaling may have potential for managing ER stress and related cellular disorders.

The endoplasmic reticulum (ER)[3] is a key site of protein synthesis and maturation, Ca^{2+} storage, and lipid biogenesis (1). There are three well-characterized ER stress sensors of the UPR: dsRNA-activated protein kinase (PKR)-like ER kinase (PERK), activating transcription factor 6 (ATF6), and inositol-requiring enzyme 1 (IRE1) (2, 3). Homeostasis of the ER is necessary for the maintenance of protein homeostasis, also called proteostasis. Overloaded unfolded or misfolded proteins are detained in the ER and cause ER stress (4, 5). To deal with the proteostasis abrogation caused by ER stress, the UPR is triggered to reduce the protein overload (4–7). However, sustained ER stress leads to various metabolic disorders associated with obesity, insulin resistance, and type 2 diabetes (8).

Upon ER stress, the UPR plays important roles in protein folding and degradation, whereas deregulation of the UPR causes metabolic disorders (2, 5, 9, 10). Specially, the ER-associated degradation (ERAD) pathway is activated by the UPR to remove unfolded or misfolded proteins to ameliorate ER stress. Besides the canonical ubiquitin–proteasome system, autophagy, a highly conserved protein degradation pathway from yeast to mammals, is considered a noncanonical ERAD pathway (11). Autophagy is a quality control system that degrades cellular content in the lysosome, in which the cytoplasmic materials are engulfed in double-membraned vesicles called autophagosomes (12, 13). The autophagosome elongation step involves two ubiquitin-like reaction processes, including formation of the Atg12–Atg5–Atg16L1 complex and conjugation of phosphatidylethanolamine to LC3 by sequential action of Atg4, Atg7, and Atg3 (14). It has been reported that genetic overexpression or the transgene of Atg5 or LC3 robustly augments autophagic activity and accelerates the elimination of substrates (15–19). On the contrary, knockdown or loss-of-function mutation of these two molecules causes autophagic degradation deficiency and substrate accumulation (20–22).

Autophagy is triggered upon ER stress to eliminate excess proteins and protect cells against metabolic damage (23–25). It has been reported that the activation of PERK and IRE1 and increased $[Ca^{2+}]_{cyt}/[Ca^{2+}]_{ER}$ mediates ER stress–induced autophagy (23, 26–28). However, the signaling pathways that couple ER stress to autophagy are not completely understood.

Calreticulin, an ER-localized Ca^{2+}-binding chaperone, is known for its roles in protein folding and quality control. Cal-

This work was supported by National Key R&D Program of China Grant 2017YFC0909601, National Natural Science Foundation of China Grants 31471129 and 31671224, Chinese Academy of Sciences Grant ZDBS-SSW-DQC-02, and the K. C. Wong Education Foundation (to Y. Li) The authors declare that they have no conflicts of interest with the contents of this article.

[1] Both authors contributed equally to this work.

[2] To whom correspondence should be addressed: Shanghai Institute of Nutrition and Health, Shanghai Institutes for Biological Sciences, Chinese Academy of Sciences, 320 Yue Yang Road, Life Science Research Building A1816, Shanghai 200031, China. Tel.: 86-21-5492-0753; E-mail: liyu@sibs.ac.cn.

[3] The abbreviations used are: ER, endoplasmic reticulum; UPR, unfolded protein response; ERAD, endoplasmic reticulum–associated degradation; LIR, LC3-interacting region; shRNA, short hairpin RNA; NC, negative control; CRT, calreticulin; GST, glutathione *S*-transferase; cDNA, complementary DNA; DMEM, Dulbecco's modified Eagle's medium; GAPDH, glyceraldehyde-3-phosphate dehydrogenase.

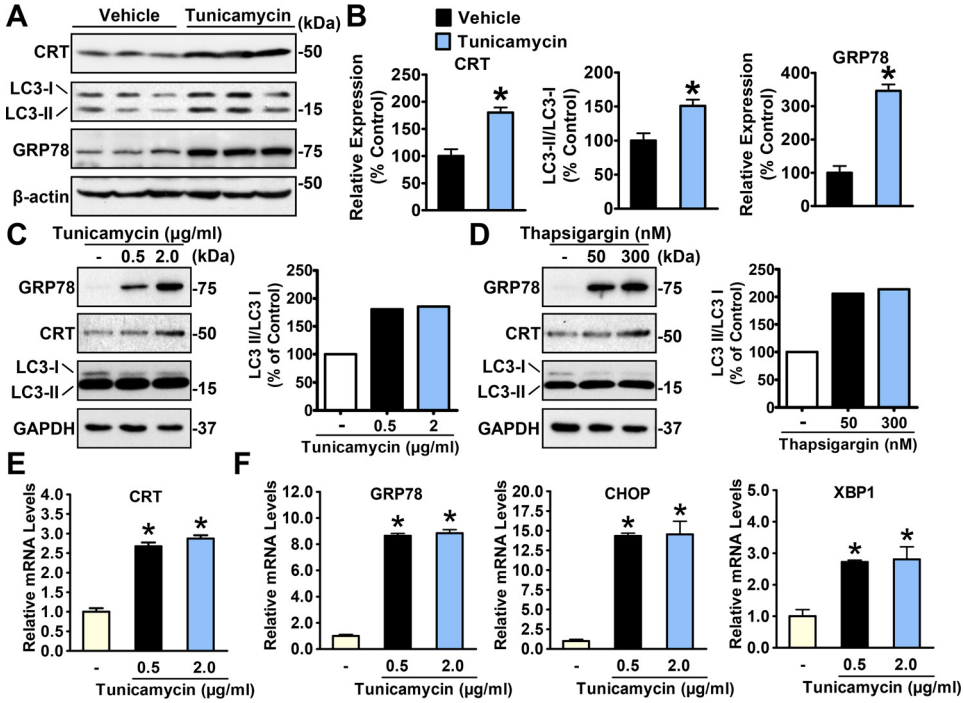

Figure 1. Calreticulin is an ER stress–inducible gene. *A*, hepatic CRT expression is increased under ER stress. Male C57BL/6 mice 8 weeks old were intraperitoneally injected with tunicamycin (1 mg/kg of body weight) or vehicle (PBS), sacrificed 48 h later for liver lysates, and assayed by immunoblotting. Three representative samples of each group are shown. *B*, densitometric quantification of expression of calreticulin, the ratio of LC3-II to LC3-I, and GRP78. *C* and *D*, the protein levels of calreticulin were increased in HeLa cells treated with gradient dosages of tunicamycin (*C*) or thapsigargin (*D*) for 16 h. The band intensity of LC3-II was quantified by densitometry and normalized to the levels of LC3-I. *E* and *F*, the relative mRNA levels of calreticulin (*E*) and UPR mediators (*F*) were increased in HeLa cells treated with gradient dosages of tunicamycin for 16 h. Data are presented as the mean ± S.E.; $n = 4$. *, $p < 0.05$ *versus* chow and vehicle.

reticulin, together with its homolog calnexin, monitors and controls the quality of newly produced glycoproteins via the "calreticulin/calnexin cycle" (29–31). In this circular supervision system, the folding levels of substrate proteins are checked to ensure that only correctly folded proteins can exit from the folding cycle within the ER membrane to the Golgi (31). However, whether and how calreticulin alleviates ER stress via other mechanisms is not understood.

Recently, we demonstrated that activation of the UPR and autophagy attenuates hepatic steatosis and insulin resistance (2, 32, 33). Here we sought to investigate the mechanisms of ER stress–induced activation of autophagy and its role in alleviating ER stress. These data suggest that ER stress induces expression of calreticulin, calreticulin stimulates the formation of autophagosome and induces autophagic flux, activation of calreticulin is sufficient to attenuate ER stress, and the LIR motif of calreticulin is of key importance in connecting autophagic machinery to inhibit ER stress. These findings provide a new insight into the molecular mechanisms of ER stress rescue signaling and may potentially become a novel therapeutic target for stress-induced disorders and proteostasis deficiencies.

Results

ER stress stimulates expression of calreticulin

Although it has been well-known that the expression of various chaperones is responsively stimulated to cope with ER stress conditions, evidence of calreticulin stimulation is scarce (34). To demonstrate whether calreticulin is stimulated by ER stress, we generated an ER stress murine model via intraperitoneal administration of an ER stress inducer, tunicamycin, and determined the hepatic expression of calreticulin. As expected, the livers of tunicamycin-treated mice showed significantly increased levels of GRP78, a representative marker of ER stress, compared with control individuals (Fig. 1*A*). The protein expression of hepatic calreticulin was increased in tunicamycin-treated mice (Fig. 1, *A* and *B*). Consistent with these findings, as shown in Fig. 1, *C–F*, calreticulin was dose-dependently up-regulated in HeLa cells treated with tunicamycin and another ER stress inducer, thapsigargin. Notably, the induction of ER stress by tunicamycin or thapsigargin was evidenced by the induction of GRP78, CHOP, and XBP1. These observations were highly consistent with previous reports (34) and led us to explore the significance of calreticulin up-regulation in response to ER stress conditions.

Calreticulin is necessary and sufficient to relieve ER stress

Given that calreticulin acts as a chaperone to assist protein folding, we hypothesized that calreticulin deficiency may lead to exacerbated ER stress. To confirm this hypothesis, calreticulin-deficient or control HeLa cells were generated using a lentivirus stably expressing calreticulin shRNA (shCRT) or negative control shRNA (shNC). As shown in Fig. 2*A*, the protein levels of calreticulin were effectively suppressed by shCRT#2 but not by the other shRNA, shCRT#1. Next, cells stably expressing shCRT#2 and shNC were treated with tunicamycin or thapsigargin, and the representative ER stress markers GRP78 and CHOP were measured. Immunoblotting and real-time quantitative PCR were performed to guarantee the efficiency of RNAi in shCRT (Fig. 2, *B*, *C*, *E*, and *F*). As expected, shCRT cells showed increased protein levels of GRP78

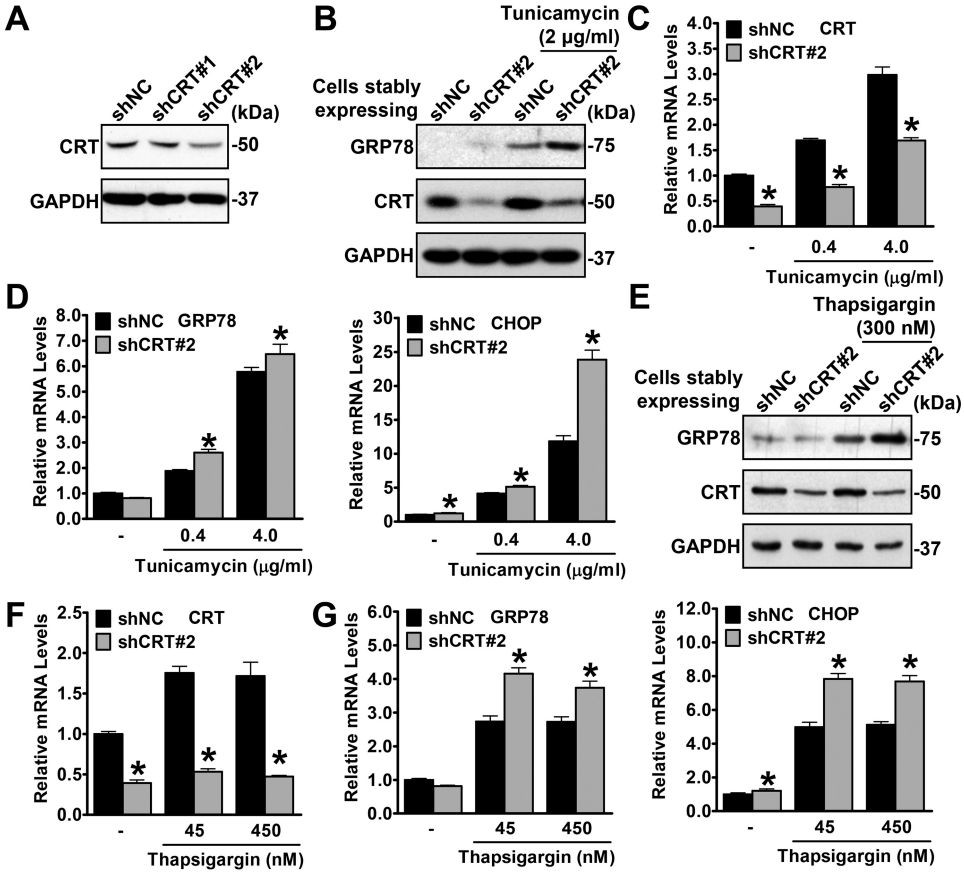

Figure 2. Calreticulin deficiency exacerbates ER stress. *A*, the protein levels of calreticulin are decreased by calreticulin knockdown using shCRT in HeLa cells. *B–D*, knockdown of calreticulin increases tunicamycin-induced ER stress. HeLa cells stably expressing shNC or shCRT were treated with vehicle (DMSO), tunicamycin, or thapsigargin with the indicated dosages for 16 h. *B*, the protein levels of GRP78 were increased in shCRT cells treated with tunicamycin. *C*, the efficiency of shCRT was confirmed by real-time qPCR. *D*, the relative mRNA levels of GRP78 and CHOP were increased in shCRT cells treated with tunicamycin. *E–G*, knockdown of calreticulin increases thapsigargin-induced ER stress. *E*, the protein levels of GRP78 were increased in shCRT cells treated with thapsigargin. *F*, the efficiency of shCRT was confirmed by real-time qPCR. *G*, the relative mRNA levels of GRP78 and CHOP were increased in shCRT cells treated with thapsigargin. Data are presented as the mean ± S.E.; $n = 4$. *, $p < 0.05$ *versus* shNC.

(Fig. 2, *B* and *E*) and increased mRNA levels of GRP78 and CHOP (Fig. 2, *D* and *G*), which indicated profound sensitivity to drug-induced ER stress.

To further illustrate the function of calreticulin in ER stress, we transiently overexpressed myc-CRT in HeLa cells, treated the cells with tunicamycin or thapsigargin, and then determined the ER stress levels by immunoblotting. In contrast to the results of knockdown experiments, a progressive decrease in GRP78 was observed when the calreticulin expression level was gradually increased (Fig. 3, *A* and *B*), suggesting a reduction of ER stress. These data support a protective role of calreticulin in response to cellular stress.

Calreticulin positively regulates autophagic flux under ER stress

We next sought to investigate the underlying mechanism of calreticulin ameliorating ER stress. In previous studies, a set of chaperones were revealed to facilitate the degradation of unfolded or misfolded proteins under stress conditions (4–7, 35, 36). Based on these discoveries, we presumed that calreticulin may be activated in response to ER stress to function similarly. Thus, we focused our study on the relationship between calreticulin and protein degradation machineries. We found that autophagic levels were elevated under the same condition,

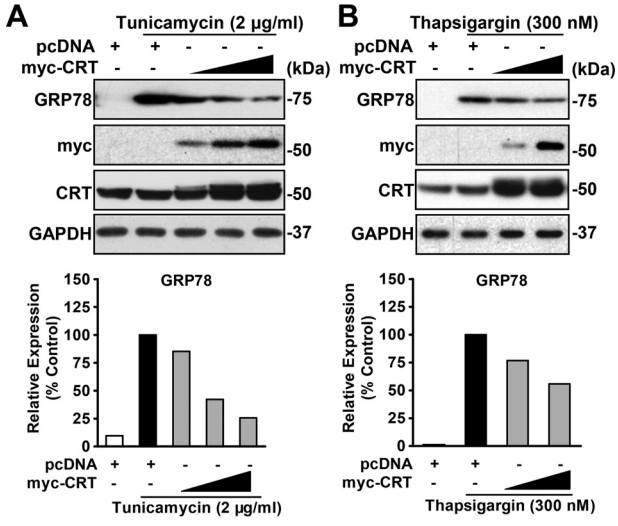

Figure 3. Calreticulin gain of function is sufficient to alleviate ER stress. *A* and *B*, overexpression of calreticulin decreased GRP78 levels in HeLa cells treated with tunicamycin (*A*) or thapsigargin (*B*). HeLa cells were transfected with gradient amounts of myc-CRT or pcDNA as a control and then treated with vehicle (DMSO), tunicamycin (2 μg/ml), or thapsigargin (300 nM) for 16 h and lysed for immunoblotting. GAPDH was used as a loading control. Densitometric quantification for expression of GRP78 was normalized to GAPDH protein levels in cell lysates.

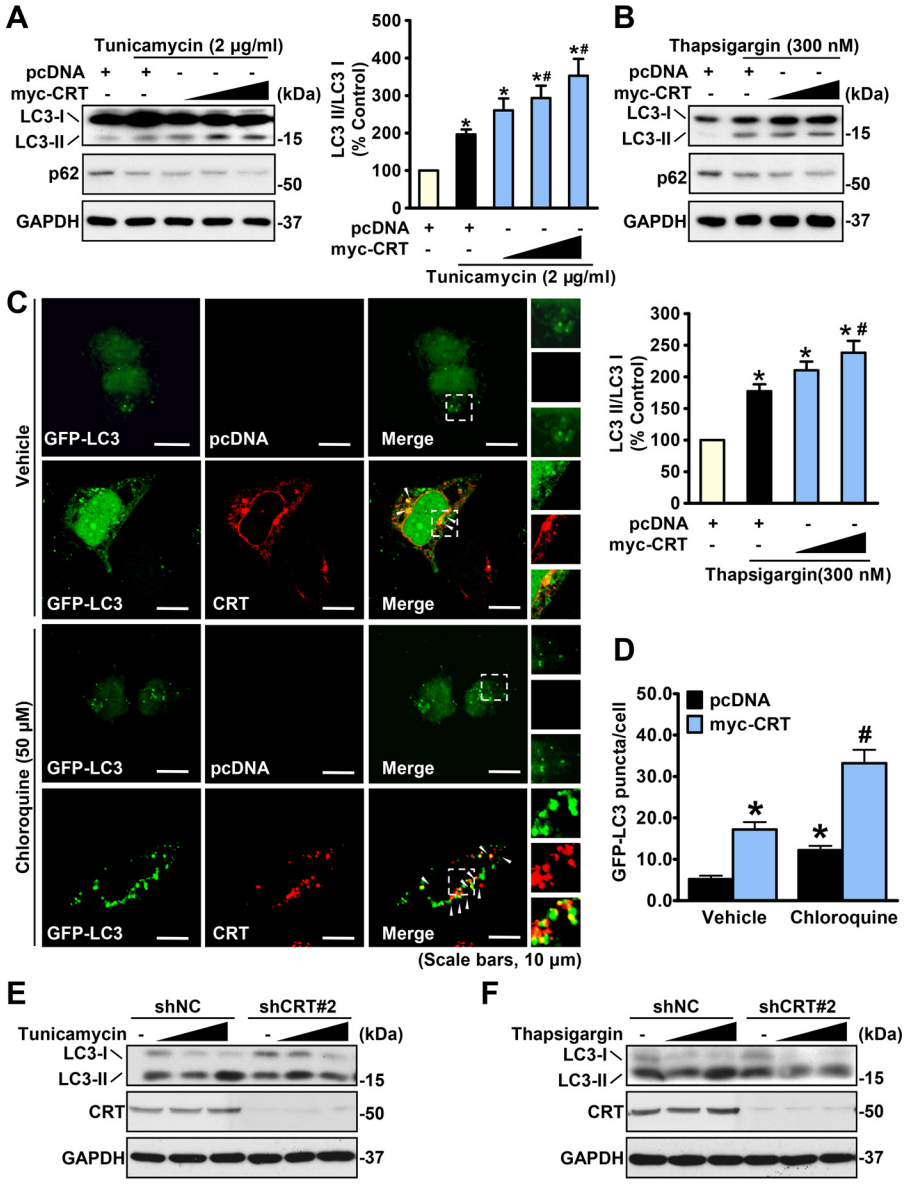

Figure 4. Calreticulin stimulates autophagic flux under ER stress. *A* and *B*, overexpression of calreticulin increased LC3-II levels in HeLa cells under ER stress. HeLa cells were transfected with gradient amounts of myc-CRT or control constructs and then treated with vehicle (DMSO), tunicamycin (2 μg/ml, *A*) or thapsigargin (300 nM, *B*) for 16 h. The band intensity of LC3-II was quantified by densitometry and normalized to the levels of LC3-I. Data are presented as the mean ± S.E.; $n = 5–6$. *, $p < 0.05$ *versus* pcDNA; #, $p < 0.05$ *versus* pcDNA and tunicamycin or thapsigargin. *C* and *D*, representative images of immunofluorescence (*scale bars* = 10 μm). HeLa cells were transfected with myc-CRT or pcDNA along with GFP-LC3 constructs to detect autophagic flux. Cells were treated with or without chloroquine (50 μM) for 10 h as indicated. myc-CRT was labeled with red fluorescence. *Arrowheads* point out the colocalized fluorescent signals. Quantification of the number of LC3 puncta is presented. Data are presented as the mean ± S.E.; $n = 5$. *, $p < 0.05$ *versus* pcDNA and vehicle; #, $p < 0.05$ *versus* pcDNA and chloroquine (50 μM). *E* and *F*, calreticulin is required for ER stress-induced autophagy in HeLa cells. Cells stably expressing shNC or shCRT were treated with vehicle (DMSO), tunicamycin (*E*), or thapsigargin (*F*) with the indicated dosages for 16 h. Immunoblots were performed.

represented by an increase in the LC3-II to LC3-I ratio (Fig. 4, *A* and *B*). Notably, the expression levels of p62 are decreased by CRT under tunicamycin and thapsigargin treatment, which is consistent with the autophagic stimulating effects of CRT. Immunofluorescence imaging manifested more LC3 puncta in the cytoplasm of calreticulin-overexpressing cells, which indicated a growth in autophagosome numbers (Fig. 4, *C* and *D*). These results indicate that calreticulin promotes autophagic flux in response to ER stress. Moreover, as shown in Fig. 4, *E* and *F*, knockdown of calreticulin decreased the conversion of LC3-I to LC3-II in HeLa cells treated with doses of tunicamycin or thapsigargin, suggesting that calreticulin is necessary for ER stress–induced autophagy. Together, these data indicate that calreticulin may couples ER stress signals to stimulate autophagy.

Calreticulin associates with LC3 through the LIR

To gain deep insight into the link between calreticulin and the autophagic degradation pathway, we studied the interaction between calreticulin and autophagic proteins. Strikingly, an evolutionarily conserved LIR, containing the motif W/Y/F*XX*L/I/V (*X* represents any residue) and existing in most LC3-interacting proteins (37), was identified in human calreticulin protein from amino acids 200 to 204 (Fig. 5*A*). To verify the interaction of calreticulin with LC3, HEK293T cells were trans-

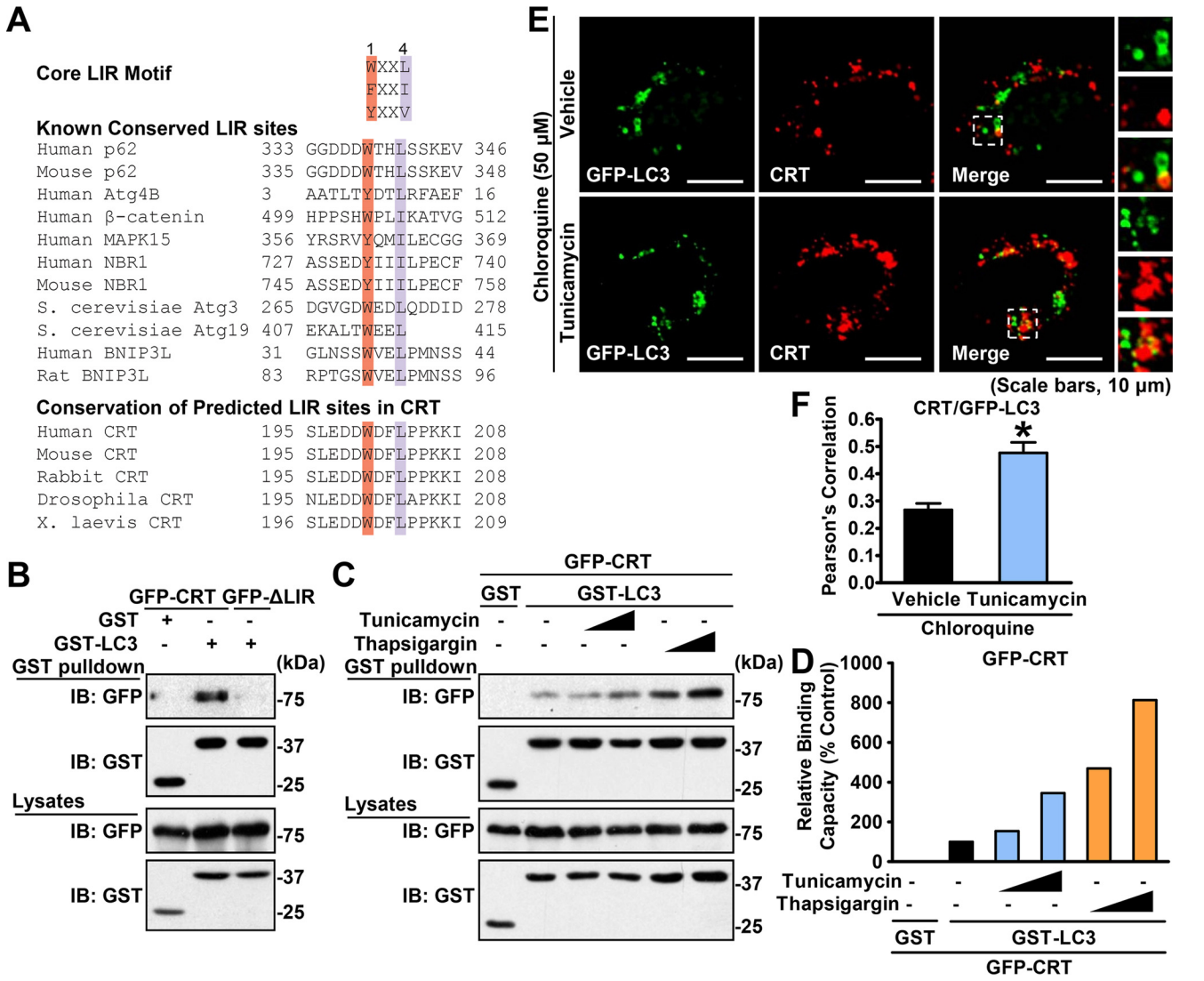

Figure 5. Calreticulin physically interacts with the autophagic protein LC3 through the LIR motif. *A*, alignment of the LIR. *B*, calreticulin, but not its ΔLIR form, physically interacted with LC3. HEK293T cells were cotransfected with the indicated constructs. GSH-agarose beads were utilized to immunoprecipitate GST-tagged proteins, and immunoblotting (*IB*) was carried out to determine the coprecipitated proteins. *C*, the interaction between calreticulin and LC3 was increased under ER stress. HEK293T cells were cotransfected with the indicated constructs and treated with vehicle (DMSO) or gradient dosages of tunicamycin or thapsigargin for 16 h. GSH-agarose beads were then utilized to immunoprecipitate GST-tagged proteins, and immunoblotting was carried out to determine the coprecipitated proteins. *D*, densitometric quantification of coprecipitated GFP-calreticulin in *C* (normalized to GFP-calreticulin protein levels in cell lysates). Shown are representative images of immunofluorescence (*scale bars* = 10 μm). *E* and *F*, the colocalization of calreticulin and LC3 is enhanced in response to tunicamycin treatment. HeLa cells were transfected with myc-CRT and GFP-LC3 constructs and treated with tunicamycin (2 μg/ml) or vehicle (DMSO) for 6 h, followed by treatment with 50 μM chloroquine for an additional 10 h as indicated. myc-CRT was labeled with red fluorescence. Confocal microscopy analysis was performed. Representative cells (*E*) and quantification of Pearson's correlation coefficient for colocalization between CRT and GFP-LC3 (*F*) are shown. Data are presented as the mean ± S.E.; $n = 5$. *, $p < 0.05$ *versus* chloroquine and vehicle.

fected with GST-tagged LC3 and GFP-tagged calreticulin constructs, and then GST pulldown was performed. As shown in Fig. 5*B*, the subsequent immunoblotting results showed a clear band of GFP-calreticulin, in contrast to the GST vector–expressing control group. To identify the binding site of calreticulin, we mutated the key residues Trp^{200} and Leu^{203} into Ala to establish the null mutation of the LIR motif (W200A, L203A) of calreticulin (calreticulin ΔLIR) and subjected the mutant to a GST pulldown test. Strikingly, the calreticulin ΔLIR mutant does not bind GST-tagged LC3 (Fig. 5*B*). These results demonstrate that the LIR motif is essential for the association between calreticulin and LC3. We supposed that the binding capacity of calreticulin with LC3 might be altered under ER stress conditions. Thus, we measured the amount of coimmunoprecipitated calreticulin under treatment with ER stress inducers. To avoid possible influence of alterations of endogenous protein expression under stress conditions, GFP-tagged calreticulin and LC3 were overexpressed in HEK293T cells, and then GST pulldown was performed. Interestingly, the association between calreticulin and LC3 was profoundly increased in a dose response to tunicamycin or thapsigargin treatment (Fig. 5, *C* and *D*). In addition, an immunofluorescence imaging analysis was performed. As shown in Fig. 5, *E* and *F*, compared with the control vehicle, treatment with tunicamycin increased the colocalization of calreticulin and LC3 under chloroquine conditions in HeLa cells. Notably, increased numbers of LC3 puncta by tunicamycin were observed.

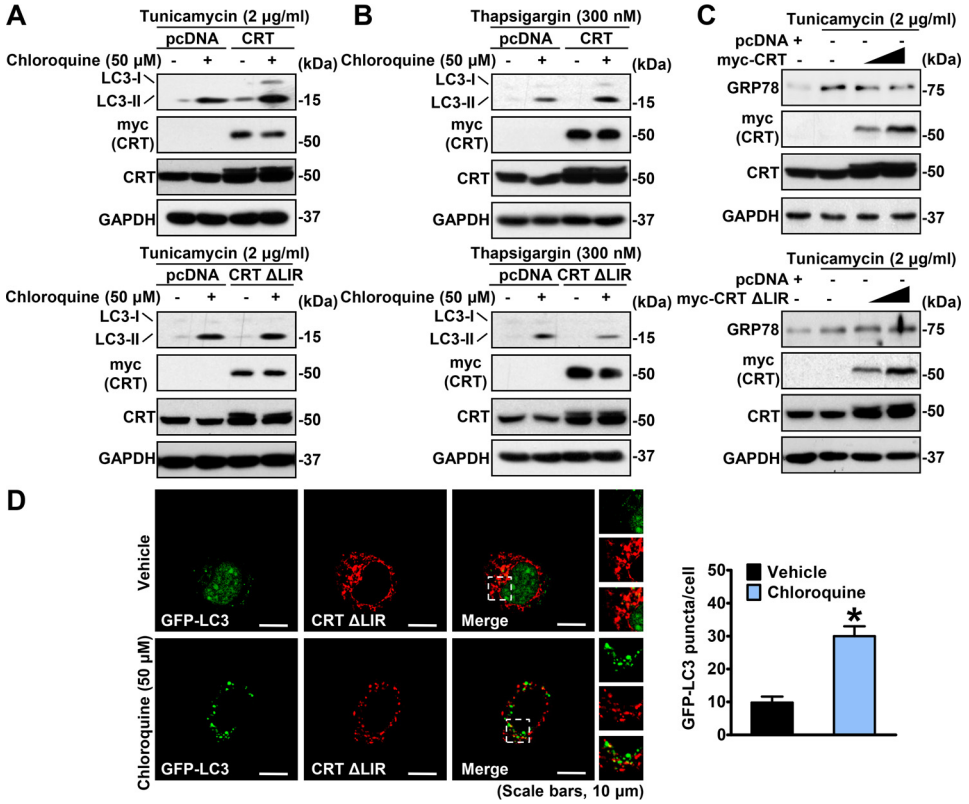

Figure 6. Mutation of the LIR motif abolishes calreticulin-mediated augmentation of autophagy and reduction of ER stress. *A* and *B*, expression of LC3-II was not promoted by calreticulin ΔLIR mutation. HeLa cells were transfected with myc-CRT or the variant ΔLIR constructs, treated with tunicamycin (2 μg/ml, *A*) or thapsigargin (300 nM, *B*) for 16 h and without or with chloroquine (50 μM) for 10 h as indicated, and then lysed for immunoblotting. *C*, drug-induced ER stress was not attenuated by overexpression of calreticulin ΔLIR mutation. HeLa cells were transfected with gradient amounts of the indicated constructs, treated with vehicle (DMSO) or tunicamycin (2 μg/ml) for 16 h, and then lysed for immunoblotting. *D*, representative images of immunofluorescence (*scale bars* = 10 μm). HeLa cells were transfected with myc-CRT ΔLIR and GFP-LC3 constructs to detect autophagic flux. myc-CRT ΔLIR was labeled with red fluorescence. Cells were treated with vehicle (DMSO) or chloroquine (50 μM) for 10 h as indicated. Then immunofluorescence was performed, and quantification of the number of LC3 puncta is presented. Data are presented as the mean ± S.E.; $n = 5$. *, $p < 0.05$ *versus* vehicle.

These results indicate that ER stress may increase the association between calreticulin and LC3 via the conserved LIR motif.

The association between calreticulin and LC3 is required for calreticulin-mediated augmentation of autophagy and reduction of ER stress

To further investigate the potential role of calreticulin/LC3 interaction in the regulation of autophagy, we expressed myc-CRT WT or the ΔLIR variant in HeLa cells and treated the cells with tunicamycin or thapsigargin. Autophagic flux assays were performed using chloroquine, a robust inhibitor of lysosomal hydrolases, to accumulate autophagosomal LC3-II. As shown in Fig. 6, *A* and *B*, in contrast to calreticulin WT–expressing cells, calreticulin-induced expression of LC3-II was largely abrogated in calreticulin ΔLIR variant–expressing cells, suggesting a dramatic decline in autophagic flux. Consistently, calreticulin ΔLIR variant–expressing cells exhibited less GFP-LC3 puncta compared with calreticulin WT–expressing cells under the same treatment in immunofluorescence imaging experiments (Figs. 4*C* and 6*D*). These data suggest that the LIR motif is required for calreticulin in the up-regulation of autophagic activity.

We next checked the ER stress levels in calreticulin ΔLIR–expressing HeLa cells compared with calreticulin WT–expressing cells under treatment with tunicamycin. The calreticulin ΔLIR–expressing cells presented a slight improvement in GRP78 signals as opposed to the attenuated bands in calreticulin WT–expressing cells (Fig. 6*C*). These findings indicate destruction of the protective role of calreticulin against ER stress conditions caused by the abolishment of calreticulin/LC3 interaction.

Taken together, we propose that up-regulation of autophagy might be the mechanism underlying calreticulin-repressed ER stress. To verify the protective role of autophagy, genetic approaches to activate or inhibit autophagy levels by overexpressing or knocking down the key autophagy components Atg5 or LC3 were performed. As shown in Fig. 7, HeLa cells with higher autophagy levels showed relatively low GRP78 levels compared with control cells, indicating their stronger tolerance of ER stress. This difference was increased under ER stress conditions. In contrast, knockdown of LC3 using shRNA caused induction of GRP78, suggesting increased ER stress. These data support the notion that autophagy activation mediates calreticulin's beneficial effects on alleviation of ER stress.

Discussion

This study demonstrates that calreticulin is a novel ER stress–inducible gene and exerts a negative feedback control system on alleviating ER stress. Mechanistically, calreticulin ameliorates ER stress in an autophagy-dependent manner, and

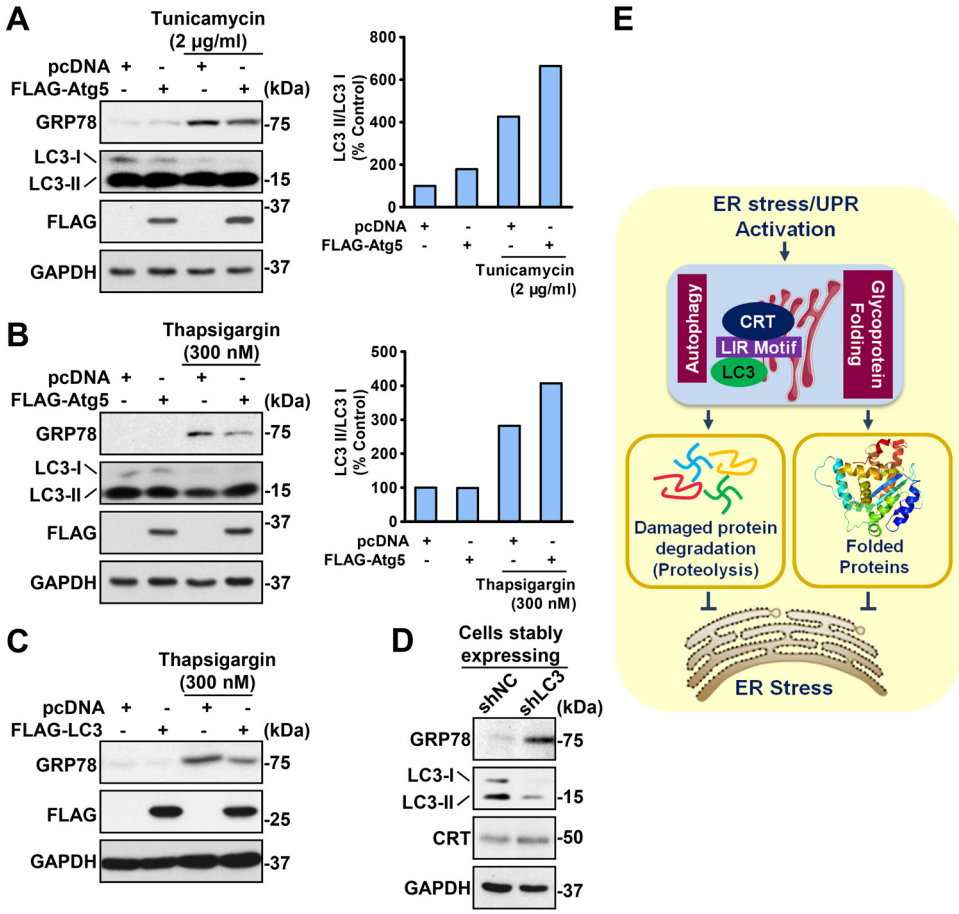

Figure 7. Autophagy protects against ER stress. *A* and *B*, overexpression of Atg5 protected against drug-induced ER stress in HeLa cells. HeLa cells were transfected with FLAG-Atg5 constructs, treated with vehicle (DMSO), tunicamycin (2 μg/ml, *A*) or thapsigargin (300 nM, *B*) for 16 h, and lysed for the indicated antibodies. The band intensity of LC3-II was quantified by densitometry and normalized to the levels of LC3-I. *C*, overexpression of LC3 protected against drug-induced ER stress in HeLa cells. HeLa cells were transfected with FLAG-LC3 constructs, treated with vehicle (DMSO) or thapsigargin (300 nM) for 16 h, and lysed for the indicated antibodies. *D*, LC3 deficiency aggravated drug-induced ER stress in HeLa cells. HeLa cells were infected with the shLC3 lentivirus and then screened with puromycin to obtain a LC3 knockdown cell line (*HeLa shLC3*). HeLa shNC and shLC3 were lysed to perform an immunoblot assay. *E*, schematic of the calreticulin–autophagy axis in the negative feedback regulation of ER stress. Calreticulin is induced by the UPR in response to ER stress. Calreticulin enhances autophagic flux to attenuate cellular stress, likely through alleviation of aberrantly folded proteins. Therapeutic approaches to activate calreticulin–autophagy signaling may have potential for treating ER stress and its related disorders.

the association between calreticulin and LC3 is critical for calreticulin's effects on augmentation of autophagy and repression of ER stress. Calreticulin-mediated regulation of autophagy and ER stress may represent a molecular mechanism by which ER stress is sensed to maintain the cellular proteostasis state.

Calreticulin acts as a critical component in the negative feedback regulation of ER stress

One of the most important findings of the study is the identification of the ER-resident chaperone calreticulin as a novel regulator of ER stress. The UPR is a critical process to restore protein homeostasis under ER stress. A variety of chaperones are increased in the ER stress–induced UPR to attenuate the stress burden (7, 38). Activation of these pathways leads to a complex cascade of downstream signaling, such as protein folding, ERAD, and autophagy (11). Consistent with a previous study (34), we found that calreticulin is up-regulated both on the transcriptional and translational levels under ER stress by *in vivo* and *in vitro* approaches. Interestingly, knockdown of calreticulin increases the expression of GRP78 in cells treated with ER stress inducers that lead to aggravation of stress burden. In contrast, calreticulin overexpression ameliorates the stress burden in parallel experiments, and these results suggest that calreticulin is necessary and sufficient to reverse the ER stress conditions. In this study, we proved that calreticulin is an UPR-induced chaperone and plays a protective role under ER stress. Further study of the upstream regulation of calreticulin is needed. It has been reported that the ATF6–NF-Y key stress factor ATF4 is known as a chaperone activator (5, 39, 40). Whether ATF6 or ATF4 plays a role in the regulation of calreticulin is of interest for investigation.

Calreticulin serves as a potent activator of autophagy

Unfolded or misfolded proteins are targeted to ERAD pathways when their conformations cannot be restored by cellular chaperones (4, 41). In addition, autophagy protects cells from adverse metabolic conditions, and it is considered a noncanonical ERAD pathway (11). Based on these facts, numerous previous studies proposed the definition of ER stress–stimulated autophagy (23–25, 42, 43), which are consistent with the observation in our study showing increased autophagy in the livers of mice treated with tunicamycin. Consistent with the previous

studies (15–22), we confirmed that modulation of cellular autophagy activity via LC3 or Atg5 is sufficient and necessary for the attenuation of ER stress.

Another novel finding of the study is that activation of calreticulin increases the autophagic levels under ER stress. In this study, we demonstrate that calreticulin increases the levels of LC3-II in cells treated with ER stress inducers, which indicates increased autophagic levels. These data suggest that calreticulin may induce autophagic machinery to alleviate misfolded proteins during ER stress and maintain a cellular proteostasis state, which is consistent with previous observations showing a protective role of autophagy against ER stress (23, 24). These results show that, in addition to retaining the misfolded glycoprotein in the folding cycle for refolding or degradation, calreticulin may alleviate cellular stress by stimulating autophagy signaling. The findings may provide a novel mechanism for chaperone-mediated activation of autophagy.

Calreticulin stimulates autophagy to suppress ER stress by enhancing its interaction with LC3

As a key autophagic protein, LC3 plays an essential role in autophagosome formation, elongation, and fusion with lysosomes (14, 44). It has been reported that autophagy receptors associate with LC3 via the conserved LIR motif (45, 46) and facilitate degradation of protein targets (47, 48). Importantly, we demonstrate that calreticulin is required for the activation of autophagy under ER stress and identified, for the first time, that calreticulin interacts with LC3 in the conserved LIR motif of calreticulin protein. Coimmunoprecipitation and immunofluorescence assays proved that calreticulin ΔLIR, a LIR motif-deficient mutant form, is not able to interact with LC3. Overexpression of calreticulin ΔLIR abolishes calreticulin-mediated autophagic flux and fails to ameliorate drug-induced ER stress. These results demonstrate that the LIR motif is necessary for the calreticulin and LC3 interaction and is of great importance for the autophagy-dependent protective role of calreticulin under ER stress. Interestingly, we noticed that the binding affinity between calreticulin and LC3 is enhanced gradually when the cellular stress levels are increased by treatment with increasing dosages of tunicamycin or thapsigargin, which may represent augmentation of calreticulin-LC3 function in alleviating ER stress. These data suggest that ER stress and autophagy are causally linked via the interaction between calreticulin and LC3.

Moreover, this study characterizes that calreticulin acts as a novel LC3-binding adapter protein and that the calreticulin–LC3 complex appears to colocalize in autophagosomes, as visualized by confocal microscopy analysis. It is likely that calreticulin facilitates nuclear export of LC3 or increases conversion of LC3-I to LC3-II, leading to induction of autophagic flux (49). The detailed mechanisms of the calreticulin–LC3 complex regarding the activation of autophagy require further investigation.

We noticed that, although HeLa cells express a significant amount of endogenous CRT, the genetic approach to activate CRT activity, such as transient transfection of the plasmid encoding CRT, is sufficient to induce autophagy and repress ER stress. During ER stress, misfolded glycoproteins are accumulated in the ER, which requires a large amount of chaperone protein such as CRT for refolding, which is supported by the observation that endogenous CRT levels are induced under tunicamycin or thapsigargin treatment. Therefore, addition of exogenous CRT protein may facilitate the axis of CRT-mediated stimulation of autophagic flux. Together, these results support a critical role of CRT in maintaining proteostasis in response to cellular stress.

In summary, this study delineates a novel mechanism of the positive regulation of calreticulin in UPR-triggered autophagy under ER stress (Fig. 7*E*). The intriguing finding of interaction between calreticulin and LC3 has provided us with new insight into the role of calreticulin, coupling ER stress to autophagy by interacting with degradation machinery. Given that activation of the UPR and autophagy protects against insulin resistance and hepatic steatosis (2, 32, 33), the finding of a calreticulin–autophagy axis in the negative feedback regulation of ER stress may provide potential new therapeutic avenues for treating stress-related disorders.

Experimental procedures

Reagents and antibodies

Tunicamycin (catalog no. T7765), thapsigargin (catalog no. T9033), and chloroquine (catalog no. C6628) were purchased from Sigma-Aldrich, and puromycin, used in stable cell line screening, was purchased from Selleck Chemicals (catalog no. S7417). The calreticulin antibody was purchased from Millipore (catalog no. MABT145), and LC3 antibodies were purchased from Novus Biologicals (catalo no. NB100-2220) and Cell Signaling Technology (catalog no. 2775). The GRP78 antibody was purchased from Santa Cruz Biotechnology (catalog no. sc-13968). The GST pulldown procedure was performed using GSH-Sepharose 4B beads (GE Healthcare Bio-Sciences) according to the manufacturer's instructions.

Plasmids and siRNA

myc-tagged calreticulin and calreticulin ΔLIR were constructed by cloning the human cDNAs into the KpnI/NotI sites of the pcDNA-myc-His B vector. GFP-tagged calreticulin and calreticulin ΔLIR were constructed by cloning the human cDNAs into the XhoI/ApaI sites of the pEGFP-N2 vector. A two-step site-directed mutagenesis process using the KOD Plus Mutagenesis kit (Toyobo, catalog no. SMK-101) was performed to generate the human calreticulin ΔLIR plasmid in which the tryptophan at the 200th amino acid and leucine at the 203rd amino acid were substituted with alanine (Trp^{200} to Ala^{200}, Leu^{203} to Ala^{203}). The following primers were used: Trp^{200} to Ala^{200}, GCTCCTTGGAAGACGATGCGGACTTCCTGCCACCC (forward) and CGGACTCCACCTGGCTGTTGTC (reverse); Leu^{203} to Ala^{203}, GCCACCCAAGAAGATAAAGGATCCT (forward) and GCGAAGTCCCAATCGTCTTCCAAGGAG (reverse). FLAG-tagged Agt5 was constructed by cloning human Agt5 cDNA into the NotI/BamHI sites of the pCMV10–3×FLAG vector. FLAG-tagged human LC3 were constructed by cloning LC3 cDNA into the SalI/NotI sites of the pcDNA-FLAG-SBP vector. The vectors pRK5-GST and pEGFP-C1 were modified and constructed to express LC3 with the SalI/NotI restriction site. The vectors psPAX2 and pMD2.G

were used to package knockdown lentiviruses. shRNAs were designed using the siRNAs above and cloned into pLKO.1, purchased from Addgene, according to the manufacturer's instructions. The sequences of CRT siRNAs were as follows (5′-3′): siCRT#1, AATCCGTCCAGAAACTGCTCC; siCRT#2, AAGGAGCAGTTTCTGGACGGA; siLC3: AGCTCATCAAGATAATTAGAA. myc-tagged calreticulin was constructed by cloning calreticulin cDNA into the KpnI/NotI sites of pcDNA. All oligonucleotides were ordered from and synthesized by Shanghai Sunny Biotechnology Co. Ltd. The plasmids were sequenced by Genewiz Co.

Cell culture and transient transfection

HeLa and HEK293T cells were maintained in complete Dulbecco's modified Eagle's medium, high-glucose (DMEM (pH 7.3), Life Technology, catalog no. 12100046) supplemented with 10% fetal bovine serum (Biological Industries, catalog no. 04-001-1ACS), 100 μg/ml penicillin, and 100 μg/ml streptomycin (Life Technology, catalog no. 15140122) at 37 °C in a humidified incubator with 5% CO_2. Cells were cultured at a confluency of about 80%. To perform transient transfection, cells were seeded on proper plates or dishes to achieve a confluency of 70–80%. Media were replaced into basal DMEM (pH 7.3) without fetal bovine serum or antibiotics. Plasmids were transfected into cells with polyethyleneimine (Sigma-Aldrich, catalog no. 408727) according to the manufacturer's instructions. Media were replaced with fresh complete DMEM 4–6 h after transfection, and cells were harvested and subjected to the following assays about 24 h after transfection.

Lentivirus production, infection, and selection

Lentiviral particles were generated as described previously (31, 50). Briefly, cells were transfected with the lentiviral transfer plasmid pCDH-CMV expressing the target gene, along with the packaging plasmids pMDLg/pRRE and pRSV-Rev (1:1 ratio) and the envelope plasmid pMD2.G using polyethyleneimine). The medium containing lentiviral particles was stored at 4 °C. For lentivirus infection, cells were cultured, treated with lentiviral particle solution, and then selected and passaged under puromycin-containing medium for 4–7 days. The resulting cells stably expressing the target gene were ready for further assays.

Animal model

Male C57BL/6 mice at 8 weeks of age were purchased from Shanghai Laboratory Animal Co. Ltd. Tunicamycin injection in mice was performed as described previously (52–54). Briefly, tunicamycin (Sigma-Aldrich, catalog no. 7765) was suspended at 0.05 mg/ml in PBS (150 mM) and injected intraperitoneally (1 μg/g of body weight). Control mice were injected with PBS. The mice were sacrificed 48 h post-injection. The livers were harvested, homogenized, and lysed for immunoblots. All mice were housed under a 12:12-h light/dark cycle at controlled temperature. All animal experimental protocols were approved by the Institutional Animal Care and Use Committee at the Shanghai Institute of Nutrition and Health, Shanghai Institutes for Biological Sciences, Chinese Academy of Sciences.

Immunoblots and GST pulldown

Immunoblot analysis was performed as described previously (55, 56). The intensity of bands was quantified using ImageJ (National Institutes of Health, Bethesda, MD). For the GST pulldown analysis, cell lysates containing overexpressed GST-tagged fusion proteins or endogenous proteins were incubated with GSH-Sepharose 4B beads (GE Healthcare Bio-Sciences) at 4 °C overnight and washed as co-immunoprecipitation. The precipitates were then analyzed by immunoblots.

RNA isolation and quantitative RT-PCR analysis

RNA isolation and reverse transcription was performed as described previously (57). The resulting cDNA was subjected to real-time PCR with gene-specific primers in the presence of SYBR Green PCR Master Mix (Applied Biosystems) using the StepOnePlus real-time PCR system (Applied Biosystems) as described previously (2). The mRNA levels of genes were normalized to those of GAPDH and presented as relative levels to control. Primers were designed using Primer3 (v. 4.0). Gene-specific primers were synthesized by Shanghai Sunny Biotechnology (Shanghai, China), and the sequences were as follows (5′-3′): calreticulin (human), CCTGCCGTCTACTTCAAGGAG (forward) and GAACTTGCCGGAACTGAGAAC (reverse); GRP78 (human), AATGACCAGAATCGCCTGAC (forward) and CGCTCCTTGAGCTTTTTGTC (reverse); XBP1 (human), GTGAGCTGGAACAGCAAGTG (forward) and CCAAGCGCTGTCTTAACTCC (reverse); CHOP (human), TGGAAGCCTGGTATGAGGAC (forward) and AAGCAGGGTCAAGAGTGGTG (reverse); GAPDH (human), TGACAACGAATTTGGCTACA (forward) and GTGGTCCAGGGGTC-TTACTC (reverse).

Fluorescence microscopy

Cells were seeded onto glass coverslips. Forty-eight hours after transfection, cells were fixed in 4% paraformaldehyde, and coverslips were mounted in ProLong Gold antifade reagent with DAPI (Life Technologies) to visualize the nuclei. Images were captured under a confocal microscope (Olympus FV1200). Quantitative analyses of colocalization were done using Image Pro Plus software (Media Cybernetics, Inc.) with calculation of Pearson's correlation coefficient (51, 58). Identical settings were used to capture images across five separate area per condition.

Statistical analysis

Data are expressed as mean ± S.E. Statistical significance was evaluated using unpaired two-tailed Student's *t* test and among more than two groups by one-way analysis of variance. Differences were considered significant at $p < 0.05$.

Author contributions—Y. Y., F. M., and Y. Li conceptualization; Y. Y., Q. S., Zhixue Liu, and Y. Li resources; Y. Y., F. M., Zhengshuai Liu, Y. Liu, and Y. Li formal analysis; Y. Y., F. M., and Y. Li validation; Y. Y., F. M., Y. Liu, and Y. Li investigation; Y. Y., F. M., Zhengshuai Liu, and Y. Li methodology; Y. Y., F. M., and Y. Li writing-original draft; Y. Y., F. M., Zhengshuai Liu, Y. Liu, and Y. Li writing-review and editing; Y. Li data curation; Y. Li software; Y. Li supervision; Y. Li funding acquisition; Y. Li visualization; Y. Li project administration.

Acknowledgments—We thank Dr. Lingling Chen (Shanghai Institutes for Biological Sciences, China) for providing lentivirus package plasmids. We also thank Yixuan Sun, Dr. Feifei Zhang, Aoyuan Cui, and Jing Gao (Shanghai Institutes for Biological Sciences, China) for technical assistance.

References

1. Cnop, M., Foufelle, F., and Velloso, L. A. (2012) Endoplasmic reticulum stress, obesity and diabetes. *Trends Mol. Med.* **18,** 59–68 CrossRef Medline
2. Chen, X., Zhang, F., Gong, Q., Cui, A., Zhuo, S., Hu, Z., Han, Y., Gao, J., Sun, Y., Liu, Z., Yang, Z., Le, Y., Gao, X., Dong, L. Q., Gao, X., and Li, Y. (2016) Hepatic ATF6 increases fatty acid oxidation to attenuate hepatic steatosis in mice through peroxisome proliferator-activated receptor α. *Diabetes* **65,** 1904–1915 CrossRef Medline
3. Rutkowski, D. T., and Kaufman, R. J. (2004) A trip to the ER: coping with stress. *Trends Cell Biol.* **14,** 20–28 CrossRef Medline
4. Chakrabarti, A., Chen, A. W., and Varner, J. D. (2011) A review of the mammalian unfolded protein response. *Biotechnol. Bioeng.* **108,** 2777–2793 CrossRef Medline
5. Hetz, C., Chevet, E., and Harding, H. P. (2013) Targeting the unfolded protein response in disease. *Nat. Rev. Drug Discov.* **12,** 703–719 CrossRef Medline
6. Hetz, C. (2012) The unfolded protein response: controlling cell fate decisions under ER stress and beyond. *Nat. Rev. Mol. Cell Biol.* **13,** 89–102 CrossRef Medline
7. Xu, C., Bailly-Maitre, B., and Reed, J. C. (2005) Endoplasmic reticulum stress: cell life and death decisions. *J. Clin. Invest.* **115,** 2656–2664 CrossRef Medline
8. Salvadó, L., Palomer, X., Barroso, E., and Vázquez-Carrera, M. (2015) Targeting endoplasmic reticulum stress in insulin resistance. *Trends Endocrinol. Metab.* **26,** 438–448 CrossRef Medline
9. Fu, S., Watkins Steven, M., and Hotamisligil, G. S. (2012) The role of endoplasmic reticulum in hepatic lipid homeostasis and stress signaling. *Cell Metab.* **15,** 623–634 CrossRef Medline
10. Ozcan, U, Cao, Q., Yilmaz, E., Lee, A. H., Iwakoshi, N. N., Ozdelen, E., Tuncman, G., Görgün, C., Glimcher, L. H., and Hotamisligil, G. S. (2004) Endoplasmic reticulum stress links obesity, insulin action, and type 2 diabetes. *Science* **306,** 457–461 CrossRef Medline
11. Senft, D., and Ronai, Z. A. (2015) UPR, autophagy, and mitochondria crosstalk underlies the ER stress response. *Trends Biochem. Sci.* **40,** 141–148 CrossRef Medline
12. Levine, B., and Kroemer, G. (2008) Autophagy in the pathogenesis of disease. *Cell* **132,** 27–42 CrossRef Medline
13. Mizushima, N., Levine, B., Cuervo, A. M., and Klionsky, D. J. (2008) Autophagy fights disease through cellular self-digestion. *Nature* **451,** 1069–1075 CrossRef Medline
14. Ravikumar, B., Sarkar, S., Davies, J. E., Futter, M., Garcia-Arencibia, M., Green-Thompson, Z. W., Jimenez-Sanchez, M., Korolchuk, V. I., Lichtenberg, M., Luo, S., Massey, D. C., Menzies, F. M., Moreau, K., Narayanan, U., Renna, M., *et al.* (2010) Regulation of mammalian autophagy in physiology and pathophysiology. *Physiol. Rev.* **90,** 1383–1435 CrossRef Medline
15. Lo, S., Yuan, S. S., Hsu, C., Cheng, Y. J., Chang, Y. F., Hsueh, H. W., Lee, P. H., and Hsieh, Y. C. (2013) Lc3 over-expression improves survival and attenuates lung injury through increasing autophagosomal clearance in septic mice. *Ann. Surg.* **257,** 352–363 CrossRef Medline
16. Pyo, J. O., Yoo, S. M., Ahn, H. H., Nah, J., Hong, S. H., Kam, T. I., Jung, S., and Jung, Y. K. (2013) Overexpression of Atg5 in mice activates autophagy and extends lifespan. *Nat. Commun.* **4,** 2300 CrossRef Medline
17. Wang, S., Li, B., Qiao, H., Lv, X., Liang, Q., Shi, Z., Xia, W., Ji, F., and Jiao, J. (2014) Autophagy-related gene Atg5 is essential for astrocyte differentiation in the developing mouse cortex. *EMBO Rep.* **15,** 1053–1061 CrossRef Medline
18. Hung, S. Y., Huang, W. P., Liou, H. C., and Fu, W. M. (2015) LC3 overexpression reduces Aβ neurotoxicity through increasing α7nAchR expression and autophagic activity in neurons and mice. *Neuropharmacology* **93,** 243–251 CrossRef Medline
19. Li, H., Peng, X., Wang, Y., Cao, S., Xiong, L., Fan, J., Wang, Y., Zhuang, S., Yu, X., and Mao, H. (2016) Atg5-mediated autophagy deficiency in proximal tubules promotes cell cycle G_2/M arrest and renal fibrosis. *Autophagy* **12,** 1472–1486 CrossRef Medline
20. Morris, S., Swanson, M. S., Lieberman, A., Reed, M., Yue, Z., Lindell, D. M., and Lukacs, N. W. (2011) Autophagy-mediated dendritic cell activation is essential for innate cytokine production and APC function with respiratory syncytial virus responses. *J. Immunol.* **187,** 3953–3961 CrossRef Medline
21. Peng, W., Du, T., Zhang, Z., Du, F., Jin, J., and Gong, A. (2015) Knockdown of autophagy-related gene LC3 enhances the sensitivity of HepG2 cells to epirubicin. *Exp. Ther. Med.* **9,** 1271–1276 CrossRef Medline
22. Pei, J., Deng, J., Ye, Z., Wang, J., Gou, H., Liu, W., Zhao, M., Liao, M., Yi, L., and Chen, J. (2016) Absence of autophagy promotes apoptosis by modulating the ROS-dependent RLR signaling pathway in classical swine fever virus-infected cells. *Autophagy* **12,** 1738–1758 CrossRef Medline
23. Ogata, M., Hino, S., Saito, A., Morikawa, K., Kondo, S., Kanemoto, S., Murakami, T., Taniguchi, M., Tanii, I., Yoshinaga, K., Shiosaka, S., Hammarback, J. A., Urano, F., and Imaizumi, K. (2006) Autophagy is activated for cell survival after endoplasmic reticulum stress. *Mol. Cell Biol.* **26,** 9220–9231 CrossRef Medline
24. Høyer-Hansen, M., and Jäättelä, M. (2007) Connecting endoplasmic reticulum stress to autophagy by unfolded protein response and calcium. *Cell Death Differ.* **14,** 1576–1582 CrossRef Medline
25. Yorimitsu, T., Nair, U., Yang, Z., and Klionsky, D. J. (2006) Endoplasmic reticulum stress triggers autophagy. *J. Biol. Chem.* **281,** 30299–30304 CrossRef Medline
26. Høyer-Hansen, M., Bastholm, L., Szyniarowski, P., Campanella, M., Szabadkai, G., Farkas, T., Bianchi, K., Fehrenbacher, N., Elling, F., Rizzuto, R., Mathiasen, I. S., and Jäättelä, M. (2007) Control of macroautophagy by calcium, calmodulin-dependent kinase kinase-β, and Bcl-2. *Mol. Cell* **25,** 193–205 CrossRef Medline
27. Kouroku, Y., Fujita, E., Tanida, I., Ueno, T., Isoai, A., Kumagai, H., Ogawa, S., Kaufman, R. J., Kominami, E., and Momoi, T. (2007) ER stress (PERK/eIF2 α phosphorylation) mediates the polyglutamine-induced LC3 conversion, an essential step for autophagy formation. *Cell Death Differ.* **14,** 230–239 CrossRef Medline
28. Fujita, E., Kouroku, Y., Isoai, A., Kumagai, H., Misutani, A., Matsuda, C., Hayashi, Y. K., and Momoi, T. (2007) Two endoplasmic reticulum-associated degradation (ERAD) systems for the novel variant of the mutant dysferlin: ubiquitin/proteasome ERAD(I) and autophagy/lysosome ERAD(II). *Hum Mol. Genet.* **16,** 618–629 CrossRef Medline
29. Gelebart, P., Opas, M., and Michalak, M. (2005) Calreticulin, a Ca^{2+}-binding chaperone of the endoplasmic reticulum. *Int. J. Biochem. Cell Biol.* **37,** 260–266 CrossRef Medline
30. Kozlov, G., Pocanschi, C. L., Rosenauer, A., Bastos-Aristizabal, S., Gorelik, A., Williams, D. B., and Gehring, K. (2010) Structural basis of carbohydrate recognition by calreticulin. *J. Biol. Chem.* **285,** 38612–38620 CrossRef Medline
31. Rutkevich, L. A., and Williams, D. B. (2011) Participation of lectin chaperones and thiol oxidoreductases in protein folding within the endoplasmic reticulum. *Curr. Opin. Cell Biol.* **23,** 157–166 CrossRef Medline
32. Sun, Y., Xia, M., Yan, H., Han, Y., Zhang, F., Hu, Z., Cui, A., Ma, F., Liu, Z., Gong, Q., Chen, X., Gao, J., Bian, H., Tan, Y., Li, Y., and Gao, X. (2018) Berberine attenuates hepatic steatosis and enhances energy expenditure in mice by inducing autophagy and fibroblast growth factor 21. *Br. J. Pharmacol.* **175,** 374–387 CrossRef Medline
33. Li, Y., Xu, S., Giles, A., Nakamura, K., Lee, J. W., Hou, X., Donmez, G., Li, J., Luo, Z., Walsh, K., Guarente, L., and Zang, M. (2011) Hepatic overexpression of SIRT1 in mice attenuates endoplasmic reticulum stress and insulin resistance in the liver. *FASEB J.* **25,** 1664–1679 CrossRef Medline
34. Schardt, J. A., Eyholzer, M., Timchenko, N. A., Mueller, B. U., and Pabst, T. (2010) Unfolded protein response suppresses CEBPA by induction of cal-

reticulin in acute myeloid leukaemia. *J. Cell Mol. Med.* **14,** 1509–1519 Medline
35. Ron, D., and Walter, P. (2007) Signal integration in the endoplasmic reticulum unfolded protein response. *Nat. Rev. Mol. Cell Biol.* **8,** 519–529 CrossRef Medline
36. Labbadia, J., and Morimoto, R. I. (2015) The biology of proteostasis in aging and disease. *Annu. Rev. Biochem.* **84,** 435–464 CrossRef Medline
37. Birgisdottir Å. B, Lamark, T., and Johansen, T. (2013) The LIR motif: crucial for selective autophagy. *J. Cell Sci.* **126,** 3237–3247 Medline
38. Hetz, C., Martinon, F., Rodriguez, D., and Glimcher, L. H. (2011) The unfolded protein response: integrating stress signals through the stress sensor IRE1α. *Physiol. Rev.* **91,** 1219–1243 CrossRef Medline
39. Harding, H. P., Zhang, Y., Zeng, H., Novoa, I., Lu, P. D., Calfon, M., Sadri, N., Yun, C., Popko, B., Paules, R., Stojdl, D. F., Bell, J. C., Hettmann, T., Leiden, J. M., and Ron, D. (2003) An integrated stress response regulates amino acid metabolism and resistance to oxidative stress. *Mol. Cell* **11,** 619–633 CrossRef Medline
40. Lange, P. S., Chavez, J. C., Pinto, J. T., Coppola, G., Sun, C. W., Townes, T. M., Geschwind, D. H., and Ratan, R. R. (2008) ATF4 is an oxidative stress-inducible, prodeath transcription factor in neurons *in vitro* and *in vivo*. *J. Exp. Med.* **205,** 1227–1242 CrossRef Medline
41. Kaufman, R. J., Scheuner, D., Schröder, M., Shen, X., Lee, K., Liu, C. Y., and Arnold, S. M. (2002) The unfolded protein response in nutrient sensing and differentiation. *Nat. Rev. Mol. Cell Biol.* **3,** 411–421 CrossRef Medline
42. Scheper, W., Nijholt, D. A., and Hoozemans, J. J. (2011) The unfolded protein response and proteostasis in Alzheimer disease: preferential activation of autophagy by endoplasmic reticulum stress. *Autophagy* **7,** 910–911 CrossRef Medline
43. Burton, L. J., Rivera, M., Hawsawi, O., Zou, J., Hudson, T., Wang, G., Zhang, Q., Cubano, L., Boukli, N., and Odero-Marah, V. (2016) Muscadine grape skin extract induces an unfolded protein response-mediated autophagy in prostate cancer cells: a TMT-based quantitative proteomic analysis. *PLoS ONE* **11,** e0164115 CrossRef Medline
44. Tanida, I., Sou, Y. S., Ezaki, J., Minematsu-Ikeguchi, N., Ueno, T., and Kominami, E. (2004) HsAtg4B/HsApg4B/autophagin-1 cleaves the carboxyl termini of three human Atg8 homologues and delipidates microtubule-associated protein light chain 3-and $GABA_A$ receptor-associated protein-phospholipid conjugates. *J. Biol. Chem.* **279,** 36268–36276 CrossRef Medline
45. Suzuki, H., Tabata, K., Morita, E., Kawasaki, M., Kato, R., Dobson, R. C., Yoshimori, T., and Wakatsuki, S. (2014) Structural basis of the autophagy-related LC3/Atg13 LIR complex: recognition and interaction mechanism. *Structure* **22,** 47–58 CrossRef Medline
46. Wild, P., McEwan, D. G., and Dikic, I. (2014) The LC3 interactome at a glance. *J. Cell Sci.* **127,** 3–9 CrossRef Medline
47. Lu, K., Psakhye, I., and Jentsch, S. (2014) Autophagic clearance of polyQ proteins mediated by ubiquitin-Atg8 adaptors of the conserved CUET protein family. *Cell* **158,** 549–563 CrossRef Medline
48. Kirkin, V., Lamark, T., Sou, Y. S., Bjørkøy, G., Nunn, J. L., Bruun, J. A., Shvets, E., McEwan, D. G., Clausen, T. H., Wild, P., Bilusic, I., Theurillat, J. P., Øvervatn, A., Ishii, T., Elazar, Z., *et al.* (2009) A role for NBR1 in autophagosomal degradation of ubiquitinated substrates. *Mol. Cell* **33,** 505–516 CrossRef Medline
49. Huang, R., Xu, Y., Wan, W., Shou, X., Qian, J., You, Z., Liu, B., Chang, C., Zhou, T., Lippincott-Schwartz, J., and Liu, W. (2015) Deacetylation of nuclear LC3 drives autophagy initiation under starvation. *Mol. Cell* **57,** 456–466 CrossRef Medline
50. Gong, Q., Hu, Z., Zhang, F., Cui, A., Chen, X., Jiang, H., Gao, J., Chen, X., Han, Y., Liang, Q., Ye, D., Shi, L., Chin, Y. E., Wang, Y., Xiao, H., *et al.* (2016) Fibroblast growth factor 21 improves hepatic insulin sensitivity by inhibiting mammalian target of rapamycin complex 1 in mice. *Hepatology* **64,** 425–438 CrossRef Medline
51. Tang, D., Kang, R., Livesey, K. M., Cheh, C.-W., Farkas, A., Loughran, P., Hoppe, G., Bianchi, M. E., Tracey, K. J., Zeh, H. J., 3rd, and Lotze, M. T. (2010) Endogenous HMGB1 regulates autophagy. *J. Cell Biol.* **190,** 881–892 CrossRef Medline
52. Nakagawa, T., Zhu, H., Morishima, N., Li, E., Xu, J., Yankner, B. A., and Yuan, J. (2000) Caspase-12 mediates endoplasmic-reticulum-specific apoptosis and cytotoxicity by amyloid-β. *Nature* **403,** 98–103 CrossRef Medline
53. Yamamoto, K., Takahara, K., Oyadomari, S., Okada, T., Sato, T., Harada, A., and Mori, K. (2010) Induction of liver steatosis and lipid droplet formation in ATF6 α-knockout mice burdened with pharmacological endoplasmic reticulum stress. *Mol. Biol. Cell* **21,** 2975–2986 CrossRef Medline
54. Zinszner, H., Kuroda, M., Wang, X., Batchvarova, N., Lightfoot, R. T., Remotti, H., Stevens, J. L., and Ron, D. (1998) CHOP is implicated in programmed cell death in response to impaired function of the endoplasmic reticulum. *Gene. Dev.* **12,** 982–995 CrossRef Medline
55. Li, Y., Xu, S., Mihaylova, M. M., Zheng, B., Hou, X., Jiang, B., Park, O., Luo, Z., Lefai, E., Shyy, J. Y., Gao, B., Wierzbicki, M., Verbeuren, T. J., Shaw, R. J., Cohen, R. A., and Zang, M. (2011) AMPK phosphorylates and inhibits SREBP activity to attenuate hepatic steatosis and atherosclerosis in diet-induced insulin-resistant mice. *Cell Metab.* **13,** 376–388 CrossRef Medline
56. Li, Y., Wong, K., Giles, A., Jiang, J., Lee, J. W., Adams, A. C., Kharitonenkov, A., Yang, Q., Gao, B., Guarente, L., and Zang, M. (2014) Hepatic SIRT1 attenuates hepatic steatosis and controls energy balance in mice by inducing fibroblast growth factor 21. *Gastroenterology* **146,** 539–549.e7 CrossRef Medline
57. Zhang, F., Hu, Z., Li, G., Huo, S., Ma, F., Cui, A., Xue, Y., Han, Y., Gong, Q., Gao, J., Bian, H., Meng, Z., Wu, H., Long, G., Tan, Y., *et al.* (2018) Hepatic CREBZF couples insulin to lipogenesis by inhibiting insig activity and contributes to hepatic steatosis in diet-induced insulin-resistant mice. *Hepatology* **68,** 1361–1375 CrossRef Medline
58. Peng, M., Yin, N., and Li, M. O. (2017) SZT2 dictates GATOR control of mTORC1 signalling. *Nature* **543,** 433–437 CrossRef Medline